

Enhancement of surface inspection by Moiré interferometry using flexible reference gratings

J. C. Martínez-Antón, H. Canabal, J. A. Quiroga, E. Bernabeu,

Departamento de Optica, Facultad de Físicas, Universidad Complutense Madrid, 28040 Madrid, SPAIN
fiopt12@emducms1.sis.ucm.es

M. Álvaro Labajo, V. Cortés Testillano

Subdirección de Investigación y Desarrollo de Tecnología y Materiales, Dirección de Proyectos y Sistemas, Construcciones Aeronáuticas, Avda. John Lennon s/n, Getafe 28906 Madrid, SPAIN

Abstract: We have extended the use of shadow Moiré technique to be implemented in simple curved surfaces by using a flexible grating. Dynamic visual inspection of surface micro-damages is significantly favored by the use of well adapted pliable gratings compared to the use of flat reference gratings. The experimental set-up consists of a plastic foil with a printed Ronchi grating stretched between three points which adapts to any cylindrical or conical convex surface independently of the relative orientation grating/surface. Static quantification of defects profiles is also possible with an attached CCD camera. Visual detection of defects in the range of $\sim 30 \mu\text{m}$ in depth is obtainable.

©2001 Optical Society of America

OCIS codes: 120.4120 Moiré techniques, 120.4630 Optical inspection, 150.3040 Industrial inspection, 120.6650 Surface measurements, figure 330.0330 Vision and color

References and links

1. O. Kafri, I. Glatt, *The Physics of Moiré Metrology*, (J. Wiley and Sons, New York, 1990)
2. K. Patorski, *Handbook of the Moiré fringe technique*, (Elsevier, Amsterdam, 1993).
3. Jae-Sun-Lim, Jongsu-Kim, Myung-Sai-Chung, "Automatic shadow moire topography: a moving-light-source method," *Opt. Lett.* **14**, 1252-1253 (1989)
4. J. M. Burg, "The metrological applications of diffraction gratings," *Prog. Opt.* **2**, 75-107 (1961)
5. H. Takasaki, "Moiré topography", *Appl. Opt.* **9**, 1467-1472 (1970)
6. J. Shamir, "Moiré gauging by projected interference fringes," *Opt. Las. Tech.* **5**, 78-86 (1973)
7. S. H. Rowe, W. T. Weldford, "Surface topography of non-optical surfaces by projected interference fringes," *Nature* **216**, 786-787 (1967)
8. X. Xinjun, J. T. Atkinson, M. J. Lalor, D. R. Burton, "Three-map absolute moire contouring," *Appl. Opt.* **35**, 6990-6995 (1996)
9. G. Mauvoisin, F. Bremand, A. Lagarde, "Three-dimensional shape reconstruction by phase-shifting shadow moire", *Appl. Opt.* **33**, 2163-2169 (1994)
10. L. Pirodda, "Shadow and projection moire techniques for absolute or relative mapping of surface shapes," *Opt.-Eng.* **21**, 640-649 (1982)
11. A. S. Redner, "Shadow-Moiré surface inspection," *Materials Evaluation* **48**, 873-878 (1990)
12. D. R. Andrews, "Shadow moire contouring of impact craters," *Opt. Eng.* **21**, 650-654 (1982)
13. J. Marasco, "Use of a curved grating in shadow Moiré," *Exp. Mech.* **15**, 464-470 (1975)
14. A. M. F. Wegdam, O. Podzimek, H. T. Bosing, "Simulation of shadow moire systems containing a curved grating surface," *Appl. Opt.* **31**, 5952-5955 (1992)
15. E. A. Patterson, M. Heredia, internal communication, European project "INDUCE" ref. BRPR-CT98-0805

1. Introduction

The shadow Moiré is a well-known technique generally used for 3-D surface profiling measurements by using a flat reference grating. It covers a wide dynamic range of heights distribution and resolution can be tailored to as good as $\sim 1 \mu\text{m}$ [1-10].

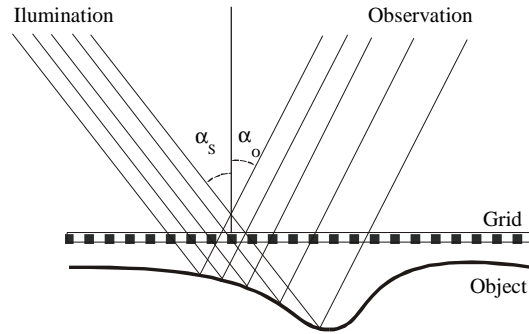


Fig. 1 Geometrical scheme of the classical shadow Moiré technique

The working principle is schematized in Fig. 1. This technique is normally implemented with a flat and binary transmitting grid (or grating). As it is well known, the height equivalent between two Moiré fringes (isotathmics) is [1-2]

$$\Delta z = d / (\tan \alpha_s + \tan \alpha_o), \quad (1)$$

where d is the grid period and α_s and α_o are the angles of source and observation directions with respect to the normal of the grating (Fig. 1). A more general expression describing the Moiré pattern may be written as

$$I = A + B \cos[2\pi z (\tan \alpha_s + \tan \alpha_o) / d], \quad (2)$$

where I is the measured radiometric magnitude, z is the height from the reference grating to the surface, A and B are respectively the offset and the modulation amplitude of the fringe pattern. A calibration from a known surface profile may serve to determine A , B and the factor $(\tan(\alpha_s) + \tan(\alpha_o)) / d$. Achievable height resolution with a digital image processing is typically $\sim 1/50$ of the fringe period. For example, for a $45^\circ/0^\circ$ configuration (which we use in our measurements) we should expect

$$\delta z = d / 50, \quad (3)$$

i.e. approximately $\sim 2 \mu\text{m}$ height sensibility for a 0.1 mm grating period. For visual inspection, the detection limit of local surface deviations is one order of magnitude worse.

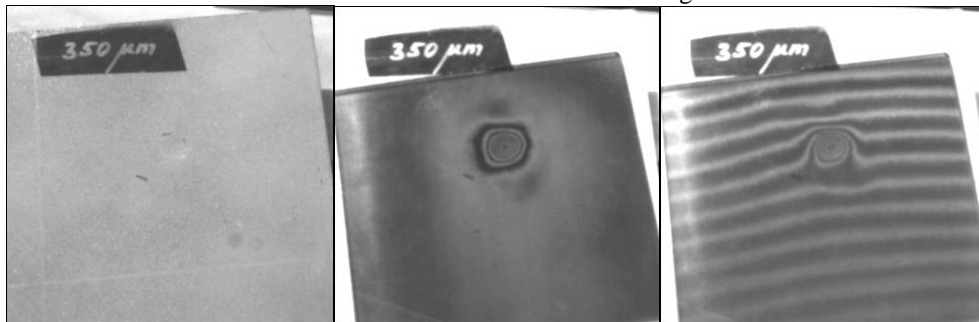


Fig. 2 a) Direct observation of a flat surface test with an indentation of $350 \mu\text{m}$ in depth practically invisible to the naked-eye. b) The same with an interposed Ronchi grating of 10 lines/mm making clearly apparent an indentation and which illustrates the enhancement of visual inspection aided by shadow Moiré. c) When the grating is tilted few millimeters over the test it appears several fringes with decreasing contrast due to diffraction. Curved surfaces produce similar patterns with low contrast which finally influences the detectability of defects and reduces the field of view drastically.

Achieving a good height resolution needs short grating periods but then, diffraction effects become predominant and spoil classical (geometrical) shadow Moiré analysis for 3-D objects other than quasi flat surfaces.

Under this context of high resolution and nearly flat surfaces, shadow Moiré is a very suitable technique applicable for thermal surface deformation analysis, for warpage in electronic boards, for checking flatness or for structural-deformation analysis, etc... Surface inspection of nearly flat surfaces for finding subsurface and impact damages has also been reported [11-12]. We are interested in developing this last application for testing curved surfaces.

Current state of the art of shadow Moiré for defect inspection works well only with quasi-flat surfaces and not so easy with curved ones. The separation of the grating probe from the surface in only few millimeters completely spoils the contrast of the Moiré fringes (see Fig. 2) due to diffraction effects. Ideally, a probe adapted to the overall curvature of the surface should reflect only the local surface deviations as wanted. This strategy has been implemented by Marasco [13] but not for surface defect inspection. Wegman *et al* [14] make a theoretical analysis of curved grating systems. However, they both used rigid curved gratings and therefore adapted only to a particular surface in a given orientation. We intend to surpass this rigid configuration by introducing a flexible grating, adaptable to different surface curvatures and for local surface deviation inspection.

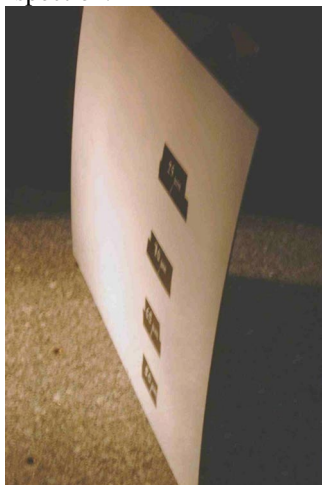


Fig. 3: Curved panel used to make the shadow Moiré tests (radius of curvature r is 2 m). It is made of composite material and typically used in aeronautic applications ($r > 1-2$ m).

The developed experimental system is able to work in convex surfaces, particularly for cylindrical and conical in shape, and independently of the radius of curvature and of the relative orientation to the surface. We have tested it on aeronautic surfaces where we find a ready application to control impact damages, bumps and corrosion lumps. It can also be extended to industrial pipes and other engineering surfaces. Generally, a surface local deviation is not necessarily a defect but, it may point out to a more critical internal damage that may need a more sophisticated analysis technique. The original goal of this work is the in-service inspection of large aeronautical structures looking for impact damages, internal delaminating (in composites) and corrosion (in metallic lap-joints).

The proposed technique can be seen as an enhancement to the simple naked-eye visual inspection by improving the detectability of surface defects by shadow Moiré. A later digital image processing would allow quantification of the different defects profile with increased resolution.

2. Adaptable gratings for curved surfaces. Results

Surface visual inspection of large areas using flat reference gratings is inappropriate. The lack of adaptation of the grating to the overall surface leads to a bad detectability of local surface deviations due to 1) the reduced field of view with contrast enough between fringes and 2) the fringes produced by curvature hinder the detection of the surface defects.

We have tried two different designs for grating adaptation to curved surfaces. We make different tests on a curved panel (Fig. 3) with several ball-impact indentations in the order of $\sim 70 \mu\text{m}$ measured by mechanical means. Probably, the real depth is less than labeled due to certain recovery of composite materials after an impact, which may last several days. The first essay consisted in using a Ronchi grating printed on a plastic foil and pressed with a semi-rigid plastic plate of around 1 mm thick as illustrated in Fig. 4. However, not fully satisfactory results were obtained in relation with visual detectability. The uniformity of the field of view was greatly increased with respect to the flat approach, but with residual Moiré fringes, difficult to avoid, due to a non ideal adaptation. These residual fringes still hinder visual reliable detectability of surface defects. Recently, a better prototype has been developed by Patterson *et al* [15] based on this symmetry. Anyhow, this configuration has still the problem of a proper alignment, i.e. the orientation of the fixture and the pressure exerted must be both aligned properly with the axis of cylindrical curvature. Any other surface different from cylindrical is impossible to adapt reasonably under this configuration.



Fig. 4: First prototype in use over a curved panel. In this case the adaptation needs a right alignment and the tensile stress on the foil is somewhat inhomogeneous. It gives poorer results than the tripod approach. We may appreciate moiré fringes in the central area due to a non-perfect adaptation disturbing a reliable detection of surface deviations.

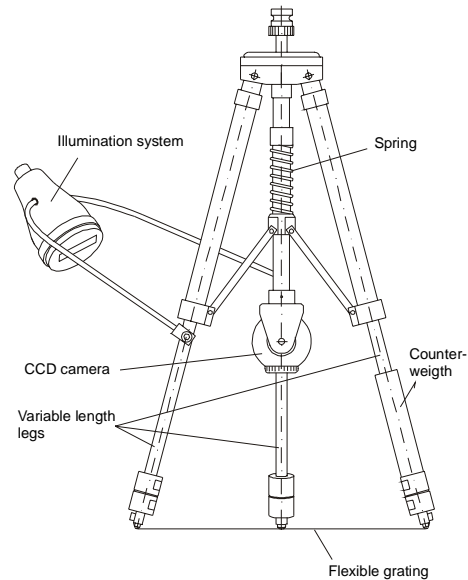


Fig. 5: Tripod solution for the adaptation of flexible gratings to curved surfaces. The grating is stretched between three contacting points. Tensile load is provided by a spring. The uniform gray appearance of the grating is a signal of good adaptation to the curved surface. Local profile deviations produce a stain like appearance. The source is a commercial 50 W halogen lamp with a dichroic reflector and a rectangle narrow aperture aligned parallel to the grating.

The proposed final solution consists of the same Ronchi grating printed on a plastic film and stretched between three points. A tripod, of the type used in photography, supports this flexible reference grating (Fig. 5). An illumination source and a CCD camera situated normal to the grating complete the setup. We have tested different periods from 4 lines/mm to 10 lines/mm with satisfactory results in all the cases cases.

The tripod approach permits a complete adaptation of the grating to convex cylindrical or conical surfaces and very approximately for shapes alike. This adaptation is independent of the relative orientation of the device supporting the grating with respect to the surface. The CCD camera installed in the middle of the tripod permits to take selected images for later quantitative processing. In Fig. 6 we show an exploration area with two different grating probes: a classical flat grating and the proposed flexible grating. The difference among them is noticeable. In static mode, the flexible approach already improves significantly the visual detectability over the flat solution on curved surfaces. Anyway, it is worth to mention that common visual detection is made dynamically, i.e. moving the grating along the surface. This characterizes the detectability in a way that favors further the tripod approach as we will see in the next section.

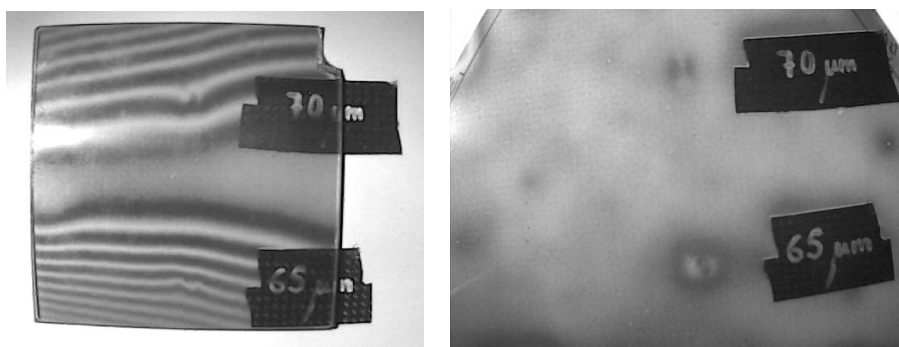


Fig. 6 Left: shadow Moiré with a curved panel and a flat grating (11 lines/mm). Right: shadow Moiré over the same area (left) with a flexible grating (10 lines/mm) mounted on the tripod support. Indentations (like a hoof track) are detected left to the numeric labels. A protrusion can be appreciated right between the labels due to a particle originated in the painting. Notice the different appearance (a white small point in the middle of the Moiré pattern).

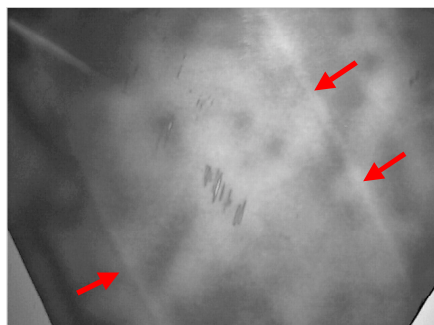


Fig. 7. Underlying structures pointed out by red arrows are readily visible through the use of the flexible grating shadow Moiré system. In the center of the image there is an area damaged by scratches.

As a consequence of several tests in real hangar conditions we have noticed that the proposed flexible shadow Moiré device can be also used to detect underlying structural details. In Fig. 7 we can appreciate seams underneath a composite painted wing invisible to the unaided eye. This feature is of special interest to locate stiffeners, reinforcements, internal corrosion, etc... in large composite structures, task difficult to do by conventional techniques usually adapted to metallic parts. These internal structures lead to small height modulations of the surface relief that are apparent under this technique.

3. Limits to the detection of surfaces defects

One of our goals was to develop a device ready for a reliable visual inspection. In practice, we have found several difficulties, which are not associated to the tripod adaptable solution but to the problem of surface deviations detection itself. Foreign inclusions associated to dirty surfaces, dust, hairs or air bubbles are the main limitation because they compete with the real local surface deviations in producing Moiré modulation patterns. That is, inclusions can be misleadingly interpreted as local surface deviations. Under this context, the static detectability of surface defects is estimated in the order of $\sim 100\ \mu\text{m}$ (depth/height) or bigger.

Fortunately, dynamic visual inspection changes the general view of this particular problem of detectability limits. Due to the nature of the flexible tripod approach, the device can be dragged along the surface to explore, i.e. translated and rotated without other limits than the surface size. This introduces a new factor related to the sensitivity of the human visual system to the movement which enhances the detection of defects. This fact, difficult to illustrate with a static picture, is the key to distinguish relevant surface deviations from inclusions. As the grating is moving along the surface, the inclusions are normally dragged too (no matter which kind of inclusion) while the real surface deviation remains in a fixed point relative to the surface. These different movement behaviors of inclusions (or false defects) and real defects improve the detectability limit (only in dynamic observation). An approximate description of the dynamic detection process is as follows: while moving the device along the surface, we should appreciate fixed Moiré stains (or partial fringe patterns) while the other Moiré stains or patterns move or simply appears and disappears randomly. To illustrate this feature of dynamic inspection we have incorporated a movie (Fig. 8). In the movie, the camera and the attached grating are the reference system and the surface moves underneath. In real inspection conditions is the opposite.



Fig. 8. (1.07 MB Movie). When moving the grating it is easier to distinguish real surface deviations from external inclusions (dirt and air bubbles) which have different behaviors. The tissue texture appreciated in the picture is due to the structural nature of the composite panel. There are two screws on the plastic grating as a reference.

Several experimental tests leads to the approximate conclusion that the minimum defect detection is in the order of $\sim 30\ \mu\text{m}$ (depth/height) independently of whether we have a theoretical much better resolution due to a high resolution grating. Finally, it is important to emphasize that digital image processing does improve height resolution but does not increase detectability of surface defects.

Other limit is the exploration of the edges and borders. Anyhow, we verified experimentally that certain “smooth” and convex edges can be reasonably inspected by leaving one or two legs of the tripod in air while maintaining a tensile strength on the grating.

Acknowledgments

This work has been developed and supported within the framework of the European Project INDUCE: Advanced Integrated NDT Concepts for Unified Life-Cycle, ref. BRPR-CT98-0805.